Calhoun
Institutional Archive of the Naval Postgraduate School

Calhoun: The NPS Institutional Archive

DSpace Repository

Faculty and Researchers | Faculty and Researchers' Publications

2014

Impact of emissions from shipping, land, and the ocean on stratocumulus cloud water elemental composition during the 2011 E-PEACE field campaign

Wang, Z.; Sorooshian, A.; Prabhakar, G.; Coggon, M.M.; Jonsson, H.H.

Elsevier Ltd.

Wang, Z., et al. "Impact of emissions from shipping, land, and the ocean on stratocumulus cloud water elemental composition during the 2011 E-PEACE field campaign." Atmospheric Environment 89 (2014): 570-580.
https://hdl.handle.net/10945/49707

This publication is a work of the U.S. Government as defined in Title 17, United

Downloaded from NPS Archive: Calhoun

http://www.nps.edu/library

Calhoun is the Naval Postgraduate School's public access digital repository for research materials and institutional publications created by the NPS community. Calhoun is named for Professor of Mathematics Guy K. Calhoun, NPS's first appointed -- and published -- scholarly author.

Dudley Knox Library / Naval Postgraduate School
411 Dyer Road / 1 University Circle
Monterey, California USA 93943

Atmospheric Environment 89 (2014) 570–580

Contents lists available at ScienceDirect

Atmospheric Environment

journal homepage: www.elsevier.com/locate/atmosenv

Impact of emissions from shipping, land, and the ocean on stratocumulus cloud water elemental composition during the 2011 E-PEACE field campaign

Z. Wang [a], A. Sorooshian [a,b,*], G. Prabhakar [b], M.M. Coggon [c], H.H. Jonsson [d]

[a] Chemical and Environmental Engineering, University of Arizona, PO Box 210011, Tucson, AZ 85721, USA
[b] Atmospheric Sciences, University of Arizona, PO Box 210081, Tucson, AZ 85721, USA
[c] Department of Chemical Engineering, California Institute of Technology, 1200 E. California Blvd., Pasadena, CA 91125, USA
[d] Center for Interdisciplinary Remotely Piloted Aircraft Studies, Naval Postgraduate School, Monterey, CA 93943, USA

HIGHLIGHTS

- Ships provide critical ocean micronutrients (e.g. P, Fe, Mn, Al, Si) to cloud water.
- Continental air masses are linked to the highest observed cloud water pH values.
- Cloud water in the study region is rarely uninfluenced by ship and land emissions.

GRAPHICAL ABSTRACT

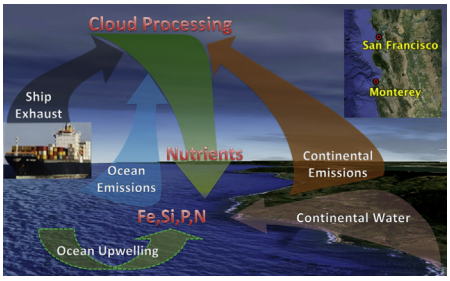

ARTICLE INFO

Article history:
Received 17 September 2013
Received in revised form
31 December 2013
Accepted 6 January 2014
Available online 22 January 2014

Keywords:
Cloud water
Shipping
Marine
Metals
Iron
Ocean
Cloud processing
Nutrients
Coastal region

ABSTRACT

This study reports on cloud water chemical and pH measurements off the California coast during the July–August 2011 Eastern Pacific Emitted Aerosol Cloud Experiment (E-PEACE). Eighty two cloud water samples were collected by a slotted-rod cloud water collector protruding above the Center for Interdisciplinary Remotely-Piloted Aircraft Studies (CIRPAS) Twin Otter in boundary layer stratocumulus clouds impacted to varying degrees by ocean-derived emissions, ship exhaust, and land emissions. Cloud water pH ranged between 2.92 and 7.58, with an average of 4.46. Peak pH values were observed north of San Francisco, simultaneous with the highest concentrations of Si, B, and Cs, and air masses originating over land. The lowest pH values were observed south of San Francisco due to ship emissions resulting in the highest concentrations of sulfate, nitrate, V, Fe, Al, P, Cd, Ti, Sb, P, and Mn. Many of these species act as important agents in aqueous-phase reactions in cloud drops and are critical ocean micronutrients after subsequent wet deposition in an ocean system that can be nutrient-limited. E-PEACE measurements suggest that conditions in the California coastal zone region can promote the conversion of micronutrients to more soluble forms, if they are not already, due to acidic cloud water conditions, the ubiquity of important organic agents such as oxalic acid, and the persistence of stratocumulus clouds to allow for continuous cloud processing.

© 2014 Elsevier Ltd. All rights reserved.

1. Introduction

Cloud droplets are critical components of the marine atmosphere due to their radiative effects and role in the geochemical cycling of nutrients. Cloud drops are produced via the nucleation of

* Corresponding author. Chemical and Environmental Engineering, University of Arizona, PO Box 210011, Tucson, AZ 85721, USA.
E-mail address: armin@email.arizona.edu (A. Sorooshian).

1352-2310/$ – see front matter © 2014 Elsevier Ltd. All rights reserved.
http://dx.doi.org/10.1016/j.atmosenv.2014.01.020

cloud condensation nuclei (CCN) and serve as a reservoir for the partitioning of soluble vapors. Cloud drops modulate CCN physicochemical properties by hosting chemical processes leading to more oxygenated species that remain in the aerosol phase upon drop evaporation. The acidity and composition of cloud water can provide insight into different air mass sources impacting clouds and the effects of wet deposition since clouds spatially redistribute nutrients and toxic pollutants.

Several aircraft studies have targeted aerosol-cloud interactions during the summertime off the California coast, which is a tailor-made venue owing to the persistence of low-level stratocumulus clouds and strong aerosol perturbations stemming from ship traffic (Chen et al., 2012). Of these experiments, some have reported data on cloud water composition with important findings being that clouds can produce secondary organic aerosol and that the region is rarely pristine but rather influenced by biogenic and anthropogenic sources (Hegg et al., 2002; Crahan et al., 2004; Straub et al., 2007). Due to limited airborne cloud water measurements off the California coast, we intend to report more recent regional data collected between July and August 2011. This study explores the effect of three distinct emission sources (ocean, ships, land) on cloud water composition.

2. Experimental methods

2.1. Field study description

The Eastern Pacific Emitted Aerosol Cloud Experiment (E-PEACE) consisted of thirty flights with the Center for Interdisciplinary Remotely-Piloted Aircraft Studies (CIRPAS) Twin Otter. Based out of Marina, California, the Twin Otter conducted ~4–4.5 h flights between 34° N–40° N and 121.5° W–125° W (Fig. 1). The goal of E-PEACE was to study aerosol-cloud-radiation interactions using a variety of observational platforms including the Twin Otter (Russell et al., 2013; Wonaschuetz et al., 2013). The current study focuses on characterizing the influence of various emissions sources on marine stratocumulus cloud water, especially exhaust from large tanker and cargo ships that frequently pass through the study region (see Fig. 1). The description of the relevant sub-set of Twin Otter measurements is provided below.

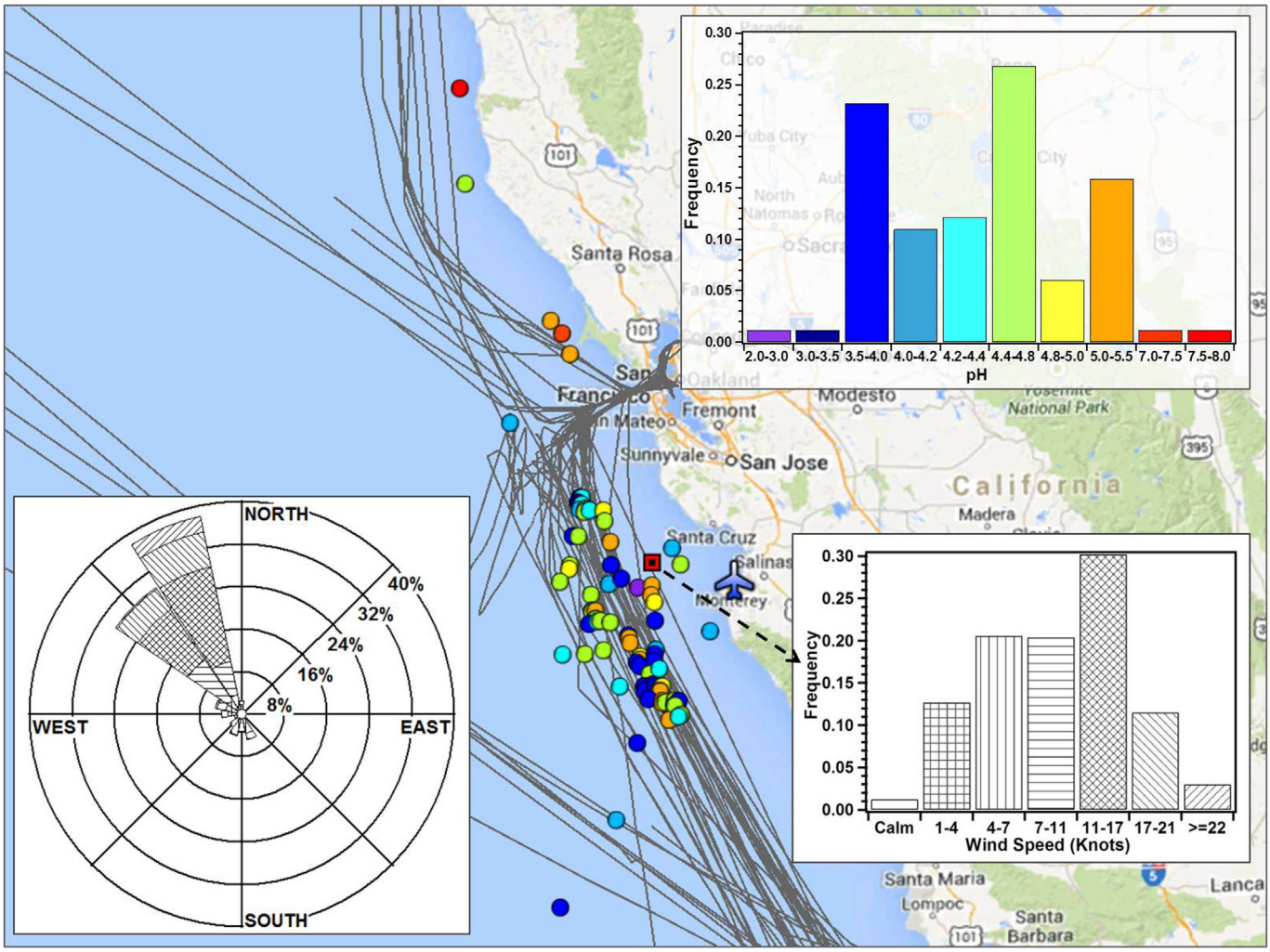

Fig. 1. Spatial distribution of cloud water pH with the insert histogram displaying the frequency of different pH values measured during E-PEACE (Note: no pHs were recorded between 5.5 and 7.0). Circular markers are color-coded by pH value consistent with the histogram color system. Solid gray lines represent the paths of 20 ships (cargo and tanker) with lengths ranging from 176 to 335 m and breadths ranging from 28 to 50 m. A 16 wind speed class wind rose and wind speed frequency table summarize the general wind conditions during the study period. They were developed using hourly wind data (1400 UTC- 2300 UTC from 8 July to 17 August) from National Data Buoy Center Station 46042 (36.785° N, 122.469° W) signified by the red square marker (www.ndbc.noaa.gov). (For interpretation of the references to color in this figure legend, the reader is referred to the web version of this article.)

2.2. Aircraft measurements

Eighty two cloud water samples were obtained with a modified Mohnen slotted-rod cloud water collector (Hegg and Hobbs, 1986). Samples were collected by insertion of the collector upwards through a port at the top of the aircraft surface when the Twin Otter was in cloud. Liquid samples were collected in detachable bottles and tested for pH immediately after collection, treated with chloroform to minimize biological processing of the samples, and then stored at a nominal 5 °C until laboratory analysis. Measurements of pH were conducted using an Oakton Model 110 pH meter calibrated with pH 4.01 and pH 7.00 buffer solutions. Eighty one samples had sufficient volume for elemental and ionic composition analysis. One fraction of the liquid volumes was analyzed with inductively coupled plasma mass spectrometry (ICP-MS), details of which are provided by Sorooshian et al. (2013). The reported measurements of all elements in each sample represent the average of three measurements. The individual measurements are typically obtained with a relative standard deviation of approximately 3% or less per sample. The minimum detection limits of the elements examined are mostly in the ppt range with a notable exception being phosphorus (P), which has a higher detection limit owing to plasma-phase interferences. Another 500 μl fraction of each cloud water sample was analyzed with ion chromatography (IC; Thermo Scientific Dionex ICS-5000 anion system with an AS11-HC 2 mm column) for major inorganic and organic acid anions.

The relative amount of Na to other constituents of sea salt (Seinfeld and Pandis, 2006) was used to calculate concentrations of non-sea salt sulfate (NSS SO_4^{2-}), non-sea salt Ca (NSS Ca), and non-sea salt bromide (NSS Br^-). This assumes that there was negligible insoluble Na. To account for the sensitivity of the ICP-MS and IC liquid-phase concentrations to cloud liquid water content (LWC), cloud water liquid concentrations were converted to air-equivalent concentrations by multiplication with the average LWC experienced during the collection of individual cloud water samples, which includes only in-cloud periods defined by a threshold LWC value of 0.02 g m^{-3}. LWC was measured by a PVM-100 probe (Gerber et al., 1994). Sub-cloud particle concentrations were obtained with a condensation particle counter (CPC 3010; TSI Inc.) and a passive cavity aerosol spectrometer probe (PCASP; PMS Inc./DMT Inc.), which have particle diameter size ranges of >10 nm and 0.1–2.6 μm, respectively. Sub-cloud is defined as being directly below cloud base with LWC <0.02 g m^{-3}.

3. Study region characteristics

Table S1 (in Supplement) summarizes cumulative E-PEACE statistics for parameters influencing the cloud water samples, including meteorological, cloud, and aerosol properties. Mean (±standard deviation) cloud base and top heights were 225 (±115) m and 587 (±131) m, respectively, with an average depth of 362 m. Sample-averaged LWC ranged between 0.07 and 0.50 g m^{-3}. Sub-cloud CPC concentrations ranged between 184 and 7143 cm^{-3}, while PCASP concentrations exhibited a smaller range between 39 and 598 cm^{-3}. The difference in the two particle concentration measurement ranges can be explained by ships emitting substantial amounts of particles with diameters less than 100 nm, which is the lower diameter cut-off size of the PCASP. Sub-cloud wind speeds measured at altitudes below 100 m ranged between 1.2 and 12.1 m s^{-1}. Sub-cloud non-refractory sub-micrometer aerosol composition during E-PEACE is summarized by Coggon et al. (2012) using an Aerodyne compact Time-of-Flight Aerosol Mass Spectrometer (C-ToF-AMS) sampling behind a total aerosol inlet (Hegg et al., 2005) and a counterflow virtual impactor in clouds (Shingler et al., 2012). Sub-cloud aerosol composition associated with the cloud water samples was dominated by organics (1.80 ± 3.30 μg m^{-3}), followed by sulfate (1.23 ± 0.82 μg m^{-3}), ammonium (0.34 ± 0.08 μg m^{-3}), chloride (0.09 ± 0.02 μg m^{-3}), and nitrate (0.05 ± 0.02 μg m^{-3}). The average ammonium-to-sulfate molar ratio was 0.68 ± 0.53, indicative of acidic sub-micrometer particles being a ubiquitous feature in the study region.

Three-day back-trajectories from the NOAA HYSPLIT model (Draxler and Rolph, 2012) are used to determine air mass origins of the 82 cloud water samples based on the sample-averaged position and time during collection of each sample. The predominant source origin of air masses influencing each of samples was to the north of the study region (Fig. S1). Trajectories are further classified into four categories based on potential land contact and the maximum level-leg sub-cloud particle concentrations: “Ship 1” = maximum CPC concentration > 14,000 cm^{-3}; “Ship 2” = 1000 cm^{-3} < maximum CPC concentration < 7000 cm^{-3}; “Land” = back-trajectory contacted land; “Marine Reference” = maximum CPC concentration < 1000 cm^{-3} “Ship 1” and “Ship 2” correspond to strong and weak ship plume influence, respectively, while “Marine Reference” corresponds to back-trajectories originating over the ocean and samples with minimal ship influence as compared to the two “Ship” categories. The category with the highest measurement frequency was “Ship 1” (34.1%), followed by “Land” (30.5%), “Ship 2” (22.0%), and “Marine Reference” (13.4%). Therefore, strong aerosol perturbations were frequently experienced in the region during E-PEACE, in contrast to “Marine Reference” conditions, which still likely is characterized by anthropogenic pollution (e.g. aged ship emissions) (Hegg et al., 2010; Coggon et al., 2012). Influence from biomass burning was not evident in E-PEACE samples.

4. Results and discussion

4.1. Cloud water pH

The average cloud water sample pH was 4.46 ± 0.70, with a range of 2.92–7.58 (Fig. 1). The most common pH observed was between 4.0–4.5 (29% of samples), followed by 4.5–5.0 (27%), and then 3.5–4.0 (23%). The pHs observed during E-PEACE are similar to those observed in marine stratocumulus clouds during the VOCALS experiment off the South American coast (range = 2.9–7.2, average = 4.3) (Benedict et al., 2012). Mean or median cloud water pH values between 4 and 5 have been observed in previous marine studies (Collett et al., 2002; Straub et al., 2007).

Cloud water pH is expected to be impacted by both LWC in clouds and chemical influences from different air mass sources. pH was moderately correlated with LWC ($r = 0.26$; $n = 78$), suggestive of higher pH with more available water. With the exception of two outlier points indicated in Fig. 2, cloud water pH generally exhibited a slight increase as a function of normalized cloud height. (Normalized cloud heights of 0 and 1 correspond to cloud base and top, respectively.) At fixed altitude and LWC, cloud water pH decreased as concentrations of two ship tracers, vanadium (V) and nitrate (Viana et al., 2009; Mueller et al., 2011), increased. The lowest pH values coincide with the “Ship 1” air type category (4.14 ± 0.51), which included samples concentrated south of San Francisco where there is extensive ship traffic (Table 2). The highest pH values are associated with the “Land” air type category (4.90 ± 0.85), coincident with the highest Si levels during E-PEACE north of San Francisco.

4.2. Chemical concentrations

The highest overall concentrations observed during E-PEACE were for Cl^- (4.31 ± 5.12 μg m^{-3}), Na (1.93 ± 2.19 μg m^{-3}), NSS SO_4^{2-}

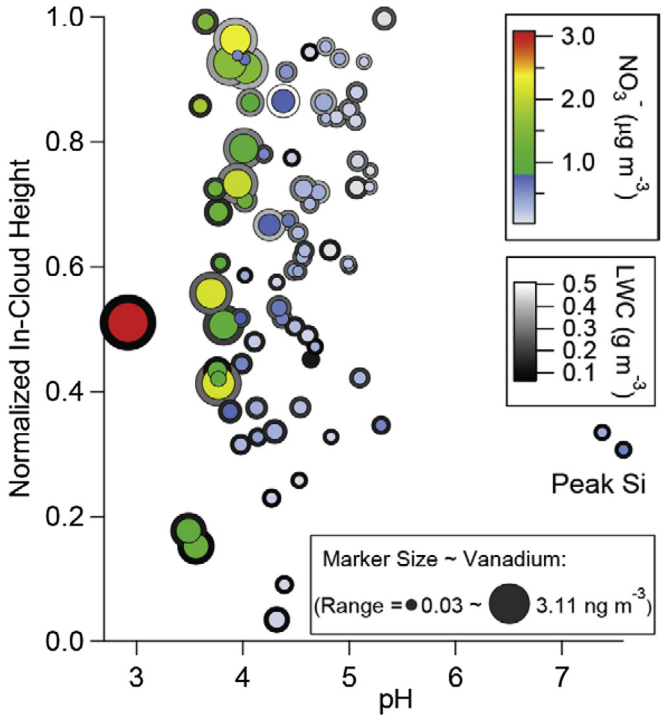

Fig. 2. Vertical distribution of cloud water pH (inner color) and LWC (outer shading). The most acidic points correspond to high levels of nitrate and vanadium from ship emissions. The highest pH points correspond to samples north of San Francisco that contained the highest Si concentrations (denoted "Peak Si"). (For interpretation of the references to color in this figure legend, the reader is referred to the web version of this article.)

(1.04 ± 0.68 μg m^{-3} with total SO_4^{2-} being 1.54 ± 1.07 μg m^{-3}), and NO_3^- (0.63 ± 0.63 μg m^{-3}) (Table 1). While Cl^- and Na are linked mainly to sea salt, sulfate has a wider variety of sources. The relative mass contributions of different sources to total sulfate are quantified using multiple linear regression (details in Supplement), where four tracers are used as independent variables: NO_3^- = "anthropogenic"; Na = "sea salt"; methanesulfonate (MSA) = "marine biogenic"; NSS Ca = "continental crustal". While Ca is emitted by other sources such as ships (Popovicheva et al., 2012), its use as a continental crustal tracer strikes a balance between achieving statistically significant results, its association with crustal matter (Johansen et al., 1999), and its higher levels in the "Land" category than the "Ship" categories in Table 2. The mass contribution percentages were found to be "anthropogenic" (37%) > "sea salt" (32%) > "marine biogenic" (26%) > "continental crustal" (6%); therefore, NSS SO_4^{2-} had an estimated contribution of 54% and 38% from anthropogenic and marine biogenic sources, respectively. These results indicate that anthropogenic pollution, mostly from shipping, was the dominant source of sulfate during E-PEACE.

Numerous other species follow in order of concentration: (i) crustal-derived elements including Mg, Si, Ca, and K (individual averages ~ 0.07–0.26 μg m^{-3}); (ii) MSA (0.06 ± 0.03 μg m^{-3}); and (iii) NO_2^- (0.03 ± 0.01 μg m^{-3}) and Br^- (0.04 ± 0.02 μg m^{-3}, with NSS Br^- being 0.03 ± 0.02 μg m^{-3}), which are two important tracers for atmospheric photochemical reactions. NO_2^- was found to be best correlated with NSS Br^- ($r = 0.81$, $n = 71$), with multiphase halogen reactions as a possible explanation (Enami et al., 2007). There are few recorded NO_2^- measurements in marine stratocumulus cloud water and its presence in clouds has previously been suggested to be due to dissolution of gaseous nitrous acid (HONO) and heterogeneous reactions of NO_2 in clouds (Lammel and Metzig, 1998).

Table 1
Cumulative summary of cloud water constituent concentrations as quantified by ICP-MS and IC in air equivalent units of μg m^{-3}. MSA refers to methanesulfonate and σ refers to standard deviation.

	Detection frequency	Min	Max	Average	σ
Cl^-	1.00	1.77E-02	2.13E+01	4.31E+00	5.12E+00
Na	1.00	1.59E-04	1.02E+01	1.93E+00	2.19E+00
NSS-SO_4^{2-}	0.96	1.06E-01	2.88E+00	1.04E+00	6.80E-01
NO_3^-	1.00	5.19E-02	3.06E+00	6.31E-01	6.25E-01
Mg	1.000	8.06E-04	1.38E+00	2.58E-01	2.92E-01
Si	0.58	1.65E-04	4.39E+00	1.92E-01	7.98E-01
Ca	0.96	4.06E-03	5.10E-01	1.04E-01	1.03E-01
K	0.86	5.27E-05	3.38E-01	6.70E-02	7.31E-02
MSA	1.00	1.32E-02	1.76E-01	5.83E-02	3.22E-02
Br^-	0.95	9.92E-03	8.84E-02	3.98E-02	2.10E-02
B	0.98	3.97E-04	1.02E+00	3.85E-02	1.58E-01
NO_2^-	1.00	9.96E-03	6.61E-02	3.16E-02	1.50E-02
F^-	0.54	8.89E-03	5.66E-02	2.32E-02	1.08E-02
P	0.04	1.69E-03	3.92E-02	1.46E-02	2.14E-02
Cd	1.00	5.57E-04	9.69E-02	7.50E-03	1.51E-02
Fe	0.75	2.07E-04	2.18E-02	3.52E-03	4.10E-03
I	0.98	7.16E-04	9.23E-03	3.13E-03	1.84E-03
Al	0.65	1.96E-05	1.67E-02	2.72E-03	3.47E-03
Cu	0.94	9.13E-06	6.57E-02	2.45E-03	8.81E-03
Zn	0.91	9.79E-06	1.45E-02	1.60E-03	2.49E-03
Sr	0.98	5.90E-05	7.73E-03	1.51E-03	1.65E-03
Mo	0.05	1.68E-06	1.82E-03	7.23E-04	8.84E-04
V	1.00	3.20E-05	3.12E-03	6.56E-04	6.69E-04
Te	0.01	3.56E-04	3.56E-04	3.56E-04	–
Mn	0.83	1.87E-06	2.23E-03	3.18E-04	4.39E-04
Ni	0.12	1.28E-05	5.92E-04	2.38E-04	2.07E-04
Ba	0.67	2.85E-06	2.26E-03	2.34E-04	4.71E-04
Se	0.57	9.21E-06	5.80E-04	1.35E-04	1.25E-04
Sb	0.84	3.59E-07	8.01E-03	1.33E-04	9.70E-04
Ag	0.02	3.21E-06	2.42E-04	1.23E-04	1.69E-04
Li	0.93	8.58E-06	6.45E-04	1.18E-04	1.08E-04
Ti	0.53	1.07E-06	5.78E-04	8.49E-05	1.31E-04
Cr	0.53	8.06E-07	3.77E-04	7.00E-05	7.46E-05
Pb	0.62	7.61E-07	3.22E-04	5.20E-05	5.97E-05
Co	0.22	9.51E-07	2.35E-04	4.21E-05	6.66E-05
Ga	0.78	2.10E-07	3.84E-04	3.29E-05	7.23E-05
Rb	1.00	8.62E-07	1.06E-04	2.65E-05	2.37E-05
As	0.20	1.15E-06	3.42E-05	9.46E-06	9.12E-06
Zr	0.73	2.17E-07	3.77E-05	5.14E-06	5.37E-06
Y	0.46	9.27E-09	3.85E-05	3.29E-06	6.48E-06
Pt	0.06	1.80E-06	4.96E-06	3.08E-06	1.20E-06
Cs	0.36	2.44E-08	1.67E-05	2.10E-06	4.15E-06

A number of other notable trace metals and metalloids were ubiquitous in the regional cloud water at lower concentrations, including Cd, V, Rb, Sr, Cu, Li, Zn, Sb, Mn, Ga, Fe, Ba, Al, Pb, Se, Ti, and Cr. These species have a variety of sources including anthropogenic emissions (e.g. combustion, smelting), biogenic emissions, soil dust, biomass burning, and sea spray (Nriagu, 1989; Al-Momani, 2003; Viana et al., 2009). Vanadium's detection in every sample provides evidence for the ubiquitous influence of ship emissions in the regional cloud water. Another common component in heavy fuel oil, nickel (Ni) (Murphy et al., 2009; Viana et al., 2009), was detected in fewer samples ($n = 10$) than V, but exhibited comparable concentrations (~0.01 ng m^{-3}). The mean V/Al mass ratio during E-PEACE was 0.67 (±0.75), which is consistent with previous values reported for oil fly ash (0.67–8.25) and two orders of magnitude larger than those of mineral and crustal dust (Sholkovitz et al., 2009).

Trace metals such as Fe, Cu, and Mn play a significant role as catalysts in cloud drop reactions, especially the conversion of SO_2 to sulfate (Alexander et al., 2009). Their frequent detection in samples (≥75%) indicates that they have a high potential to participate in such aqueous-phase processes in the regional clouds. Phosphorus is a critical ocean micronutrient that was detected in only three

Table 2
Average values of numerous parameters as a function of air mass type. To the bottom are ICP-MS and IC cloud water concentrations reported in units of μg m^{-3}. Bold and italicized cloud water concentrations coincide with the air type category for which a particular sub-set of constituents exhibit their peak concentrations. The classification method of the four air mass types is provided in Section 3.

	Marine Reference			Ship I			Ship II			Land		
	Avg	σ	n	Avg	σ	n	Avg	σ	n	Avg	σ	n
pH	4.17	0.47	11	4.14	0.51	27	4.45	0.44	17	4.90	0.85	27
LWC (g m^{-3})	0.18	0.06	11	0.21	0.11	27	0.20	0.07	17	0.27	0.10	27
Wind (m s^{-1})	9.01	3.37	11	3.96	2.93	27	8.81	2.03	17	7.41	2.88	27
PCASP (cm^{-3})	292	153	11	288	153	27	275	94	17	283	123	25
CPC (cm^{-3})	575	223	11	1585	1520	27	885	618	17	1246	1340	27
Cl^-	***8.87E+00***	***7.16E+00***	***11***	1.58E+00	3.10E+00	26	3.95E+00	3.86E+00	17	5.32E+00	5.01E+00	27
Na	***4.02E+00***	***3.12E+00***	***11***	6.07E-01	6.76E-01	26	1.80E+00	1.53E+00	17	2.43E+00	2.28E+00	27
Mg	***5.33E-01***	***4.14E-01***	***11***	8.40E-02	9.04E-02	26	2.42E-01	2.07E-01	17	3.22E-01	3.08E-01	27
Ca	***1.93E-01***	***1.45E-01***	***11***	4.77E-02	4.15E-02	25	9.74E-02	7.37E-02	16	1.24E-01	1.11E-01	26
K	***1.42E-01***	***9.25E-02***	***10***	2.19E-02	2.49E-02	19	5.40E-02	5.02E-02	16	7.93E-02	7.67E-02	25
MSA	***7.37E-02***	***3.83E-02***	***11***	4.71E-02	3.15E-02	26	4.59E-02	1.76E-02	17	7.06E-02	3.16E-02	27
Br^-	***4.99E-02***	***2.70E-02***	***11***	2.96E-02	1.81E-02	23	3.75E-02	2.12E-02	17	4.61E-02	1.68E-02	26
I	***3.54E-03***	***1.53E-03***	***11***	3.22E-03	2.29E-03	26	2.49E-03	1.08E-03	16	3.27E-03	1.83E-03	26
Sr	***3.06E-03***	***2.38E-03***	***11***	5.68E-04	5.00E-04	24	1.36E-03	1.17E-03	17	1.81E-03	1.74E-03	27
Se	***1.89E-04***	***1.27E-04***	***10***	6.76E-05	5.44E-05	11	1.47E-04	1.03E-04	9	1.42E-04	1.56E-04	16
Li	***1.58E-04***	***8.67E-05***	***10***	7.35E-05	6.37E-05	21	9.97E-05	5.11E-05	17	1.48E-04	1.49E-04	27
Rb	***4.69E-05***	***2.95E-05***	***11***	1.15E-05	9.19E-06	26	2.45E-05	1.65E-05	17	3.38E-05	2.62E-05	27
Si	2.01E-02	4.65E-02	8	2.92E-02	4.71E-02	17	1.55E-02	3.37E-02	10	***6.83E-01***	***1.52E+00***	***12***
B	2.88E-02	6.84E-02	11	3.63E-03	1.80E-03	24	1.64E-02	4.97E-02	17	***8.74E-02***	***2.60E-01***	***27***
NO_2^-	2.48E-02	7.73E-03	11	3.07E-02	1.80E-02	26	2.87E-02	1.11E-02	17	***3.70E-02***	***1.50E-02***	***27***
F^-	2.09E-02	3.46E-03	8	2.10E-02	1.10E-02	13	2.02E-02	7.87E-03	12	***3.09E-02***	***1.40E-02***	***11***
Zn	1.01E-03	1.32E-03	11	1.14E-03	1.55E-03	24	1.85E-03	2.13E-03	15	***2.17E-03***	***3.60E-03***	***24***
Ni	–	–	–	1.95E-04	1.99E-04	7	5.92E-04	–	1	***2.11E-04***	***7.98E-05***	***2***
Cr	5.15E-05	3.52E-05	8	3.84E-05	3.36E-05	14	6.28E-05	1.19E-04	9	***1.25E-04***	***6.38E-05***	***12***
Pb	3.13E-05	1.86E-05	10	4.77E-05	4.20E-05	17	5.92E-05	8.99E-05	11	***6.87E-05***	***6.99E-05***	***12***
Co	–	–	–	2.21E-05	2.00E-05	6	4.33E-05	7.82E-05	5	***5.83E-05***	***8.63E-05***	***7***
As	1.28E-05	7.19E-06	6	4.08E-06	9.18E-07	2	3.20E-06	7.73E-07	4	***1.34E-05***	***1.46E-05***	***4***
Cs	1.21E-06	2.48E-06	8	5.11E-07	5.16E-07	5	8.89E-07	1.70E-06	10	***6.64E-06***	***7.12E-06***	***6***
NSS-SO_4^{2-}	1.31E+00	8.30E-01	11	***1.34E+00***	***1.07E+00***	***25***	8.66E-01	4.52E-01	16	8.95E-01	5.49E-01	27
NO_3^-	7.49E-01	5.51E-01	11	***9.76E-01***	***8.17E-01***	***26***	3.53E-01	2.68E-01	17	4.26E-01	4.24E-01	27
Fe	2.82E-03	1.26E-03	10	***5.34E-03***	***5.38E-03***	***20***	1.75E-03	1.37E-03	12	3.08E-03	4.17E-03	19
Al	1.50E-03	1.60E-03	10	***3.46E-03***	***4.74E-03***	***20***	1.52E-03	1.26E-03	8	3.18E-03	3.00E-03	15
V	4.26E-04	2.41E-04	11	***1.15E-03***	***8.59E-04***	***26***	3.99E-04	2.30E-04	17	4.32E-04	4.95E-04	27
Mn	2.24E-04	7.31E-05	10	***4.31E-04***	***5.49E-04***	***21***	1.68E-04	1.60E-04	13	3.40E-04	5.07E-04	23
Ba	1.04E-04	8.56E-05	10	***3.60E-04***	***5.82E-04***	***20***	6.53E-05	6.48E-05	8	2.42E-04	5.47E-04	16
Cd	6.09E-03	4.64E-03	11	5.06E-03	3.42E-03	26	***1.01E-02***	***2.33E-02***	***17***	8.81E-03	1.83E-02	27
Cu	9.56E-04	2.50E-03	11	7.55E-04	1.30E-03	25	***5.67E-03***	***1.75E-02***	***14***	2.97E-03	7.74E-03	26
Sb	1.16E-05	1.16E-05	10	2.20E-05	2.69E-05	20	***5.80E-04***	***2.14E-03***	***14***	1.54E-05	2.34E-05	24
Ti	2.99E-05	1.37E-05	6	7.24E-05	1.35E-04	16	***1.27E-04***	***1.42E-04***	***7***	1.02E-04	1.50E-04	14

samples, which may have been due partly to a high detection limit in the ICP-MS for this particular element. Mercury (Hg) was only detected in one sample indicating that it is not ubiquitous in the regional cloud water.

4.3. Spatial distribution and common sources of cloud water species

To categorize species into sub-groups based on common sources, a correlation matrix was produced (Table S2) and revealed the existence of three general sub-sets of species. The sub-groups are related to three major sources (land, ship, ocean) and are consistent with the species in Table 2 that peak in concentration for these air type categories previously defined in Section 3. The impacts of these emissions on cloud water are discussed below.

4.3.1. Ocean-derived emissions

Species in the "Marine Reference" category exhibiting statistically significant correlations with each other's concentrations include Cl^-, Na, Mg, Ca, K, Br^-, Rb, Sr, Li, and MSA. With the exception of MSA, these species are positively correlated with low-level wind speed (<100 m; Table S2), coinciding with the highest sub-cloud PCASP concentrations (Table S1) and consequently the greatest sea spray influence. These species exhibited their highest concentrations south of San Francisco during E-PEACE (Figs. 3 and S2).

An example of a research flight (RF) with a clear signature of ocean-derived emission influence in cloud water was RF23 on 9 August 2011 (flight tracks shown in Fig. 4a). The computed back-trajectories and wind directions measured by the Twin Otter in flight show that the air mass probed during this flight was transported south along the California coast (Fig. 4c). This flight fits in the "Marine Reference" air type category as it had minimal influence from fresh ship emissions based on sub-cloud particle concentrations (CPC < 1000 cm^{-3}) and relatively low concentrations of V (0.20 ± 0.04 ng m^{-3}) as compared to the average value for the "Ship 1" category (1.15 ± 0.86 ng m^{-3}). Typical "Land" tracers like Si, B and Cs were either below detection limits or greatly reduced as compared to the "Land" category (Table 2). The low-level wind speed throughout this flight was 9.51 ± 1.85 m s^{-1}, which was enhanced relative to the E-PEACE (Table S1) and "Marine Reference" average (Table 2). Therefore, the potential for ocean-derived emissions was high during this flight, while land and ship emission influences were relatively low. Concentrations of the species that are most enhanced in the "Marine Reference" category of Table 2 (i.e. Na, Mg, Cl^-, K, NSS SO_4^{2-}, Sr, Br, Rb) exhibit near their highest campaign-wide levels during this flight (Table 3). Se, I, and MSA were similarly enhanced during this flight with average concentrations of 0.12 ± 0.12 ng m^{-3}, 4.34 ± 0.41 ng m^{-3}, and 0.09 ± 0.02 μg m^{-3}, respectively. The back-trajectories passing

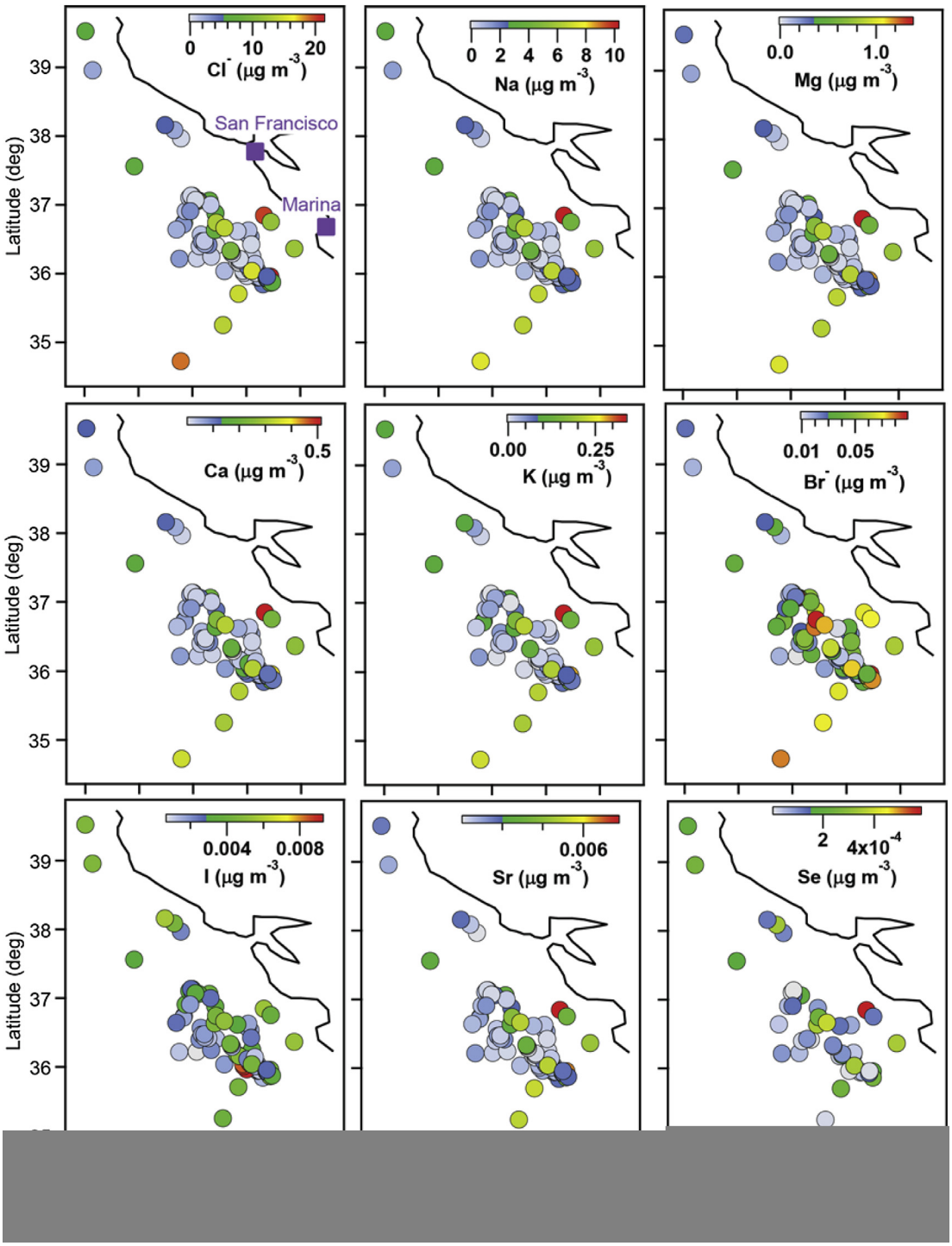

Fig. 3. Spatial distribution of cloud water constituents linked to ocean-derived emissions (MSA and Rb are shown in Fig. S2).

south through the dense area of ship traffic between San Francisco and Marina suggest that these samples were influenced to some extent by aged ship emissions. This may have contributed to the high NSS SO_4^{2-} levels in addition to ocean-derived dimethylsulfide (DMS) emissions.

4.3.2. Ship emissions

Species in the two "Ship" air type categories exhibiting statistically significant correlations with each other's concentrations include V, Al, Cd, Fe, Ti, Sb, Ba, Mn, NO_3^-, and NSS SO_4^{2-}. The influence of ship traffic on cloud water composition is most evident in the area south of San Francisco, as shown by peak concentrations of ship tracer species (e.g. V, NSS SO_4^{2-}) in Fig. 5. The "Ship 1" category includes the highest concentrations for Fe, V, Al, Mn, NSS SO_4^{2-}, and NO_3^-, while the "Ship 2" category includes maximum levels for Ti, Cu, Cd, and Sb (Table 2). Previous work has detected the majority of these species in ship exhaust particles (Xie et al., 2007; Popovicheva et al., 2009, 2012; Viana et al., 2009). It is uncertain as to what the dominant source was for the four elements with maximum concentrations in the "Ship 2" category, but one

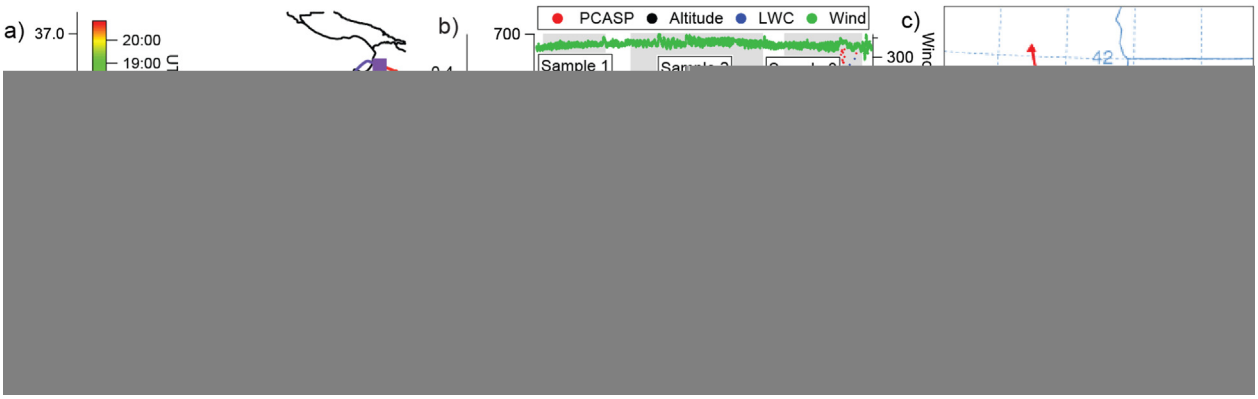

Fig. 4. (a) Flight path on 9 August 2011 (RF23) with arrows showing the spatial extent across where each of the three cloud water samples were obtained. (b) Time trace of PCASP particle concentrations (D_p ~ 0.1–2.6 μm), cloud LWC, wind direction, and Twin Otter altitude. Shaded regions correspond to when the three samples were collected. PCASP concentrations are not shown in cloud due to potential drop shatter issues. (c) 24-hr HYSPLIT back-trajectories ending at the vicinity where the three samples were collected (green = 1500 m; blue = 500 m; red = 100 m). (For interpretation of the references to color in this figure legend, the reader is referred to the web version of this article.)

possibility is coincident emissions from other sources such as the ocean or land.

RF16 on 29 July 2011 provides an example of strong influence by cargo ship emissions in an area southwest of Marina where majority of cloud water samples during E-PEACE were collected, including those during RF23 (Fig. 6). Sub-cloud PCASP concentrations were enhanced on this day relative to RF23 due to the strong influence of ship emissions, which is reflected in the lower cloud water pHs (3.70–3.95; Table 3). Sub-cloud wind speeds were low (2.94 ± 1.07 m s^{-1}), suggestive of suppressed marine-derived emissions relative to RF23. While the four RF16 samples were collected in nearly the same area as those in RF23, the concentrations of the following marine-derived tracer constituents were significantly reduced: Na, Mg, Ca, K, Cl^-, Sr, Br, Rb. Cloud water NSS SO_4^{2-} levels during RF16 (2.69 ± 0.19 μg m^{-3}) were higher than those in RF23 (1.53 ± 0.26 μg m^{-3}) due to the added influence of fresh ship exhaust superimposed on ocean-derived sources. Cloud water constituents that were enhanced in concentration by at least a factor of 1.6 during RF16 versus RF23 included Si, P, Mn, Fe, Ti, V, NSS SO_4^{2-}, and still others not shown in Table 3 (NO_3^-, Al, Ba, Cd, Sb, Pb, I). These data further support that ship emissions are a major source of the aforementioned species in cloud water.

4.3.3. Land emissions

The species with concentrations exhibiting the highest correlations in the "Land" air type category include Si, B, and Cs. They similarly peak in concentration adjacent to coastline north of San Francisco (Fig. 5). Their documented sources include crustal matter and fly ash (Gioda et al., 2008; Furutani et al., 2011). Toxic elements including Pb, As, Cr, Zn, and Ni also peak in concentration in the "Land" category indicative of land sources; these species have been shown to be enriched in continental crustal matter as a result of anthropogenic activity (Sorooshian et al., 2012).

RF28 demonstrates the impact of land emissions on regional cloud water. Four samples were collected with the first and last in the same areas, and the middle two in similar areas (Fig. 7a). The samples collected later in the day (Samples 3 and 4) exhibit major chemical differences as compared to the first two samples (Table 3): cloud water pH increased from 4.68–5.38 in the first two samples to 7.38–7.58 for the last two samples, while LWC was relatively constant. Air mass back-trajectories show that the marine boundary layer was likely impacted by land emissions during this flight, especially the third sample at cloud-relevant altitudes (Fig. 7b/c). PCASP concentrations were highest during RF28 in clear air when the Twin Otter ascended over the land area at the northernmost part of the flight track, which impacted the air mass arriving at the cloud region where Samples 3–4 were collected (Fig. 7c).

Cloud water during this flight was not impacted heavily by fresh ship emissions owing to higher pH (4.68–7.58) and lower V (≤0.18 ng m^{-3}), NSS SO_4^{2-} (≤0.85 μg m^{-3}), and sub-cloud CPC particle concentrations (max CPC ~ 707–1039 cm^{-3}) as compared to the two "Ship" categories in Table 2. Ocean-derived emissions were unlikely to have been as large an influence on these samples as compared to other flights and especially the "Marine Reference" samples owing to reduced levels of Na, Mg, Cl^-, K, SO_4^{2-}, Sr, Br, and Rb. The most significant difference in this flight relative to the other

Table 3
Chemical and pH measurements for cloud water during three case flights (29 July 2011, RF16; 9 August 2011, RF23; 16 August 2011, RF28). The "Air Mass Type" corresponds to the categories from Table 2. "Norm" refers to normalized cloud height. Blank cells indicate concentrations below detection limits.

	Air Mass Types	Norm. cloud height	μg m^{-3}									ng m^{-3}								
			PH	Si	Na	Mg	B	Ca	K	Cl^-	NSS SO_4^{2-}	Sr	P	Mn	Fe	Br	Rb	Ti	V	Al
RF16	Ship I	0.41	3.77	0.11	0.36	0.07	0.01	0.11	0.01	0.57	2.88	0.86	2.82	2.23	18.16	4.16	0.03	0.05	2.35	9.98
		0.56	3.70	0.09	0.32	0.06	0.01	0.10	0.01	0.49	2.80	0.69		1.66	14.33	4.17	0.01	0.55	2.13	9.25
		0.73	3.95	0.17	0.56	0.06	0.01	0.15	0.04	0.52	2.64	0.69	39.22	1.87	21.76	4.57	0.04	0.12	1.96	15.43
		0.96	3.93	0.06	0.31	0.05	0.01	0.10	0.01	0.51	2.46	0.64		1.60	13.69	4.01	0.02	0.05	2.19	16.71
RF23	Marine Reference	0.93	4.02		6.50	0.85	0.01	0.30	0.20	13.50	1.35	4.96		0.12	1.90	27.79	0.07		0.23	0.69
		0.94	3.95		7.36	0.97	0.01	0.35	0.23	18.82	1.83	5.68		0.05	0.90	34.63	0.08		0.15	0.00
		0.78	4.20	0.004	4.55	0.61	0.01	0.21	0.14	9.85	1.40	3.46		0.28	3.20	17.07	0.05		0.23	1.28
RF28	Land	0.11	5.38	0.11	0.35	0.03	0.21	0.02	0.01	0.60	0.45	0.13		0.09		16.78	0.01		0.18	0.00
		0.47	4.68	0.13	1.33	0.16	0.23	0.07	0.04	2.48	0.63	0.89		0.25	1.18	16.30	0.03		0.12	5.95
		0.31	7.58	4.39	2.93	0.29	0.92	0.13	0.09	5.82	0.82	1.56	1.69	1.31	1.87	11.26	0.05	0.19	0.15	0.85
		0.33	7.38	3.41	1.69	0.11	1.02	0.06	0.04	2.40	0.85	0.50		0.34	1.30	5.71	0.04	0.21	0.13	0.61

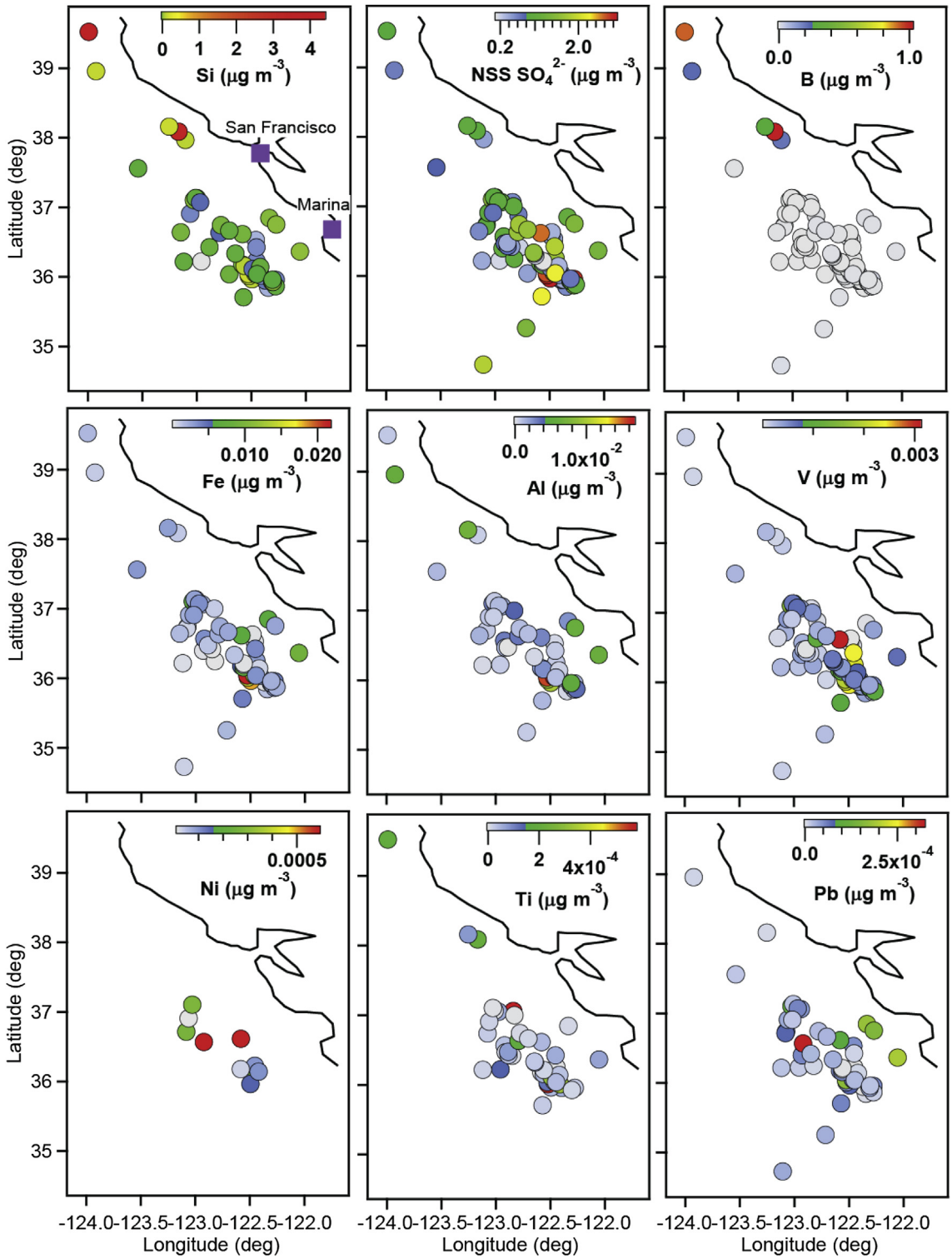

Fig. 5. Spatial distribution of selected cloud water constituents linked to ship emissions that are higher in concentration south of San Francisco. Note that both Si and B are also linked to land-derived emissions and thus are enhanced in concentration north of San Francisco (Cs is shown in Fig. S2).

E-PEACE flights are the high Si concentrations in the final two samples (3.41–4.39 μg m^{-3}), which the data indicate were more influenced by land emissions. Either one or both of the final two samples exhibited at least twice as high a concentration for the following constituents as compared to the first two samples: Si, Na, B, K, Cl^{-}, P, Mn, Ti, Li, Cr, Cs, Cu, Mo, and Co. Chemical ratios in RF28 samples differ widely from those reported for soil (Seinfeld and Pandis, 2006): (ratio of Sample 3–4 average in RF28 versus value from Seinfeld and Pandis, 2006): Si:Al = 5355 vs 4.63, Fe:Al = 2.12 vs 0.53, Fe:Ca = 0.02 vs 2.77, Mg:Na = 0.08 vs 1.00. The exact source of the emissions that impacted these samples is unknown, but a possibility is the influence of fly ash, which is known to be enriched with silica oxide, which can partly help explain the high level of Si relative to other common crustal elements such as Al and Fe.

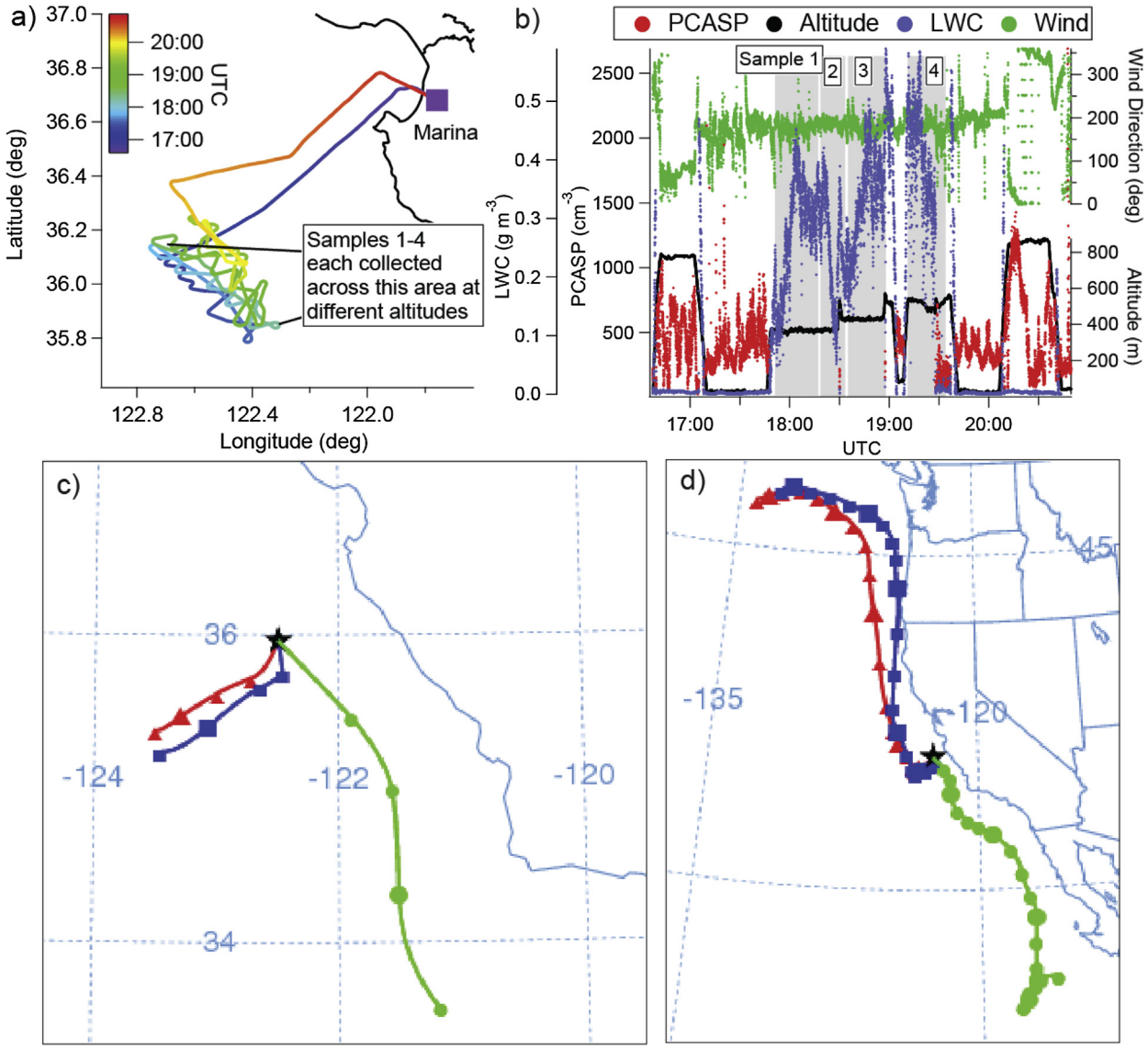

Fig. 6. (a) Flight path on 29 July 2011 (RF16) with line indicators showing the spatial extent across where each of the four cloud water samples were obtained. Samples were collected across the same general area, but with each successive one being at a higher altitude in cloud. (b) Time trace of PCASP particle concentrations (D_p ~ 0.1–2.6 μm), cloud LWC, wind direction, and Twin Otter altitude. Shaded regions correspond to when the four samples were collected. (c) 24-hr and (d) 120-hr HYSPLIT back-trajectories ending at the point of each of the four samples for UTC 18:00 (green = 1500 m; blue = 500 m; red = 100 m). (For interpretation of the references to color in this figure legend, the reader is referred to the web version of this article.)

4.4. Nutrients in cloud water

Depending on time and location, parts of the California coastal region can be characterized by HNLC-like (high-nutrient, low-chlorophyll) conditions with iron limiting primary production (Johnson et al., 1997; Kirchman et al., 2000). A number of cloud water constituents studied, including Fe, P, Mn, Si, and Al, are of significance with regard to their role in increasing ocean biota productivity (Moore et al., 1984; Singh et al., 2008) and thus impacting the global C, N and P cycles (Zhuang et al., 1990; Jickells et al., 2005; Krishnamurthy et al., 2009). Sources of nutrient fluxes to coastal ocean regions such as the study region include ocean upwelling, continental water inputs, and atmospheric wet and dry deposition (Galloway et al., 2004; Capone and Hutchins, 2013). E-PEACE measurements reveal the impact of different emissions sources on the atmospheric deposition pathway of relevant micronutrients, especially iron, which can assist with promoting ocean productivity. When comparing the average concentration of these nutrients in three previously-defined air type source categories ("Ship 1", "Land", and "Marine Reference") to the sum of the average concentration of the three categories (P excluded due to limited data), Fe, Mn, and Al are similar in that shipping is their main source (55%, 47%, 53%, respectively) followed by continental air (30%, 41%, 36%), and background marine conditions (15%, 12%, 11%). On the other hand, Si has its main contribution from continental air (93%), followed by shipping (6%), and background marine conditions (1%). Therefore, a key finding from E-PEACE is that shipping and continental pollution inject nutrients into cloud water that can deposit to the ocean via precipitation and promote productivity.

The impact of micronutrients in cloud water on ocean biota, especially via uptake by phytoplankton, depends on their solubility. Dust-derived forms of these nutrients are typically insoluble, but their acid mobilization in polluted conditions can

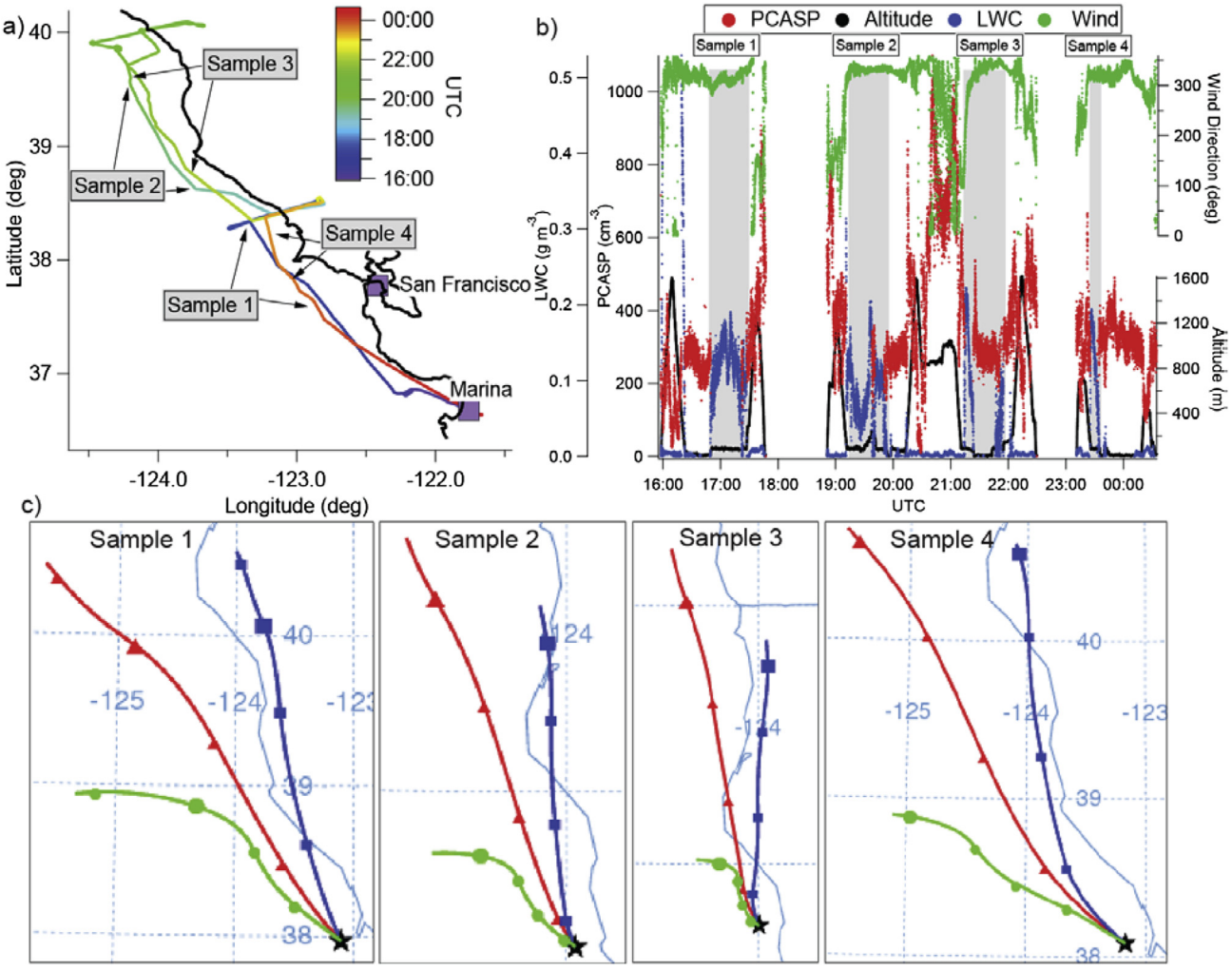

Fig. 7. (a) Flight path on 16 August 2011 (RF28) with arrows showing the spatial extent across which each of the four cloud water samples were obtained. (b) Time trace of PCASP particle concentrations (D_p ~ 0.1–2.6 μm), cloud LWC, wind direction, and Twin Otter altitude. Shaded regions correspond to when the four samples were obtained. (c) 24-hr HYSPLIT back-trajectories ending at the point of each of the four samples (green = 1500 m; blue = 500 m; red = 100 m). (For interpretation of the references to color in this figure legend, the reader is referred to the web version of this article.)

promote their availability in a soluble form (Zhuang et al., 1992). Meskhidze et al. (2005) suggested that advection of Asian dust plumes over the Pacific Ocean and exposure to SO_2 promotes acid mobilization and production of soluble Fe. Photochemical and cloud processing also can modify solubility of these nutrients (Luo et al., 2005; Shi et al., 2009); for example, reactions of ferric Fe with organics such as oxalic acid, which is abundant in the study region (Sorooshian et al., 2010, 2013), can produce soluble Fe (Zuo and Hoigne, 1992). Our observations suggest that conditions in the California coastal zone region are ideal for the conversion of nutrients emitted from land sources and ships to a more soluble form, if they are not already, due to acidic cloud water conditions promoted by ship emissions, abundance of organics such as oxalic acid, and the persistence of stratocumulus clouds to allow for continuous cloud processing. Further work is warranted to examine the nature of these micronutrients in the study region, including their solubility.

5. Conclusions

This work reports on the acidity and composition of 82 cloud water samples collected on-board the CIRPAS Twin Otter during the 2011 E-PEACE campaign. The main findings of this work include the following:

(1) Cloud water pH in the region ranged widely between 2.92 and 7.58 and was strongly influenced by ship emissions (low pH) and land-derived air masses (high pH).
(2) Marine-derived emissions lead to strong enhancements in the following constituents: Na, Mg, Cl^-, K, Sr, Br^-, Rb, Se, I, MSA. Ship emissions are estimated to have been a larger contributor to NSS SO_4^{2-} (~54%) as compared to marine biogenic emissions (~38%).
(3) Ship emissions resulted in cloud water with enhanced levels of V, Fe, Mn, P, Ti, Cd, Al, Ba, Sb, Pb, I, Se, NO_3^-, and NSS SO_4^{2-}. Ships are shown to be an even stronger source for such ocean micronutrients (P, Fe, Mn, Al) in the region as compared to land emissions. Highly acidic cloud water due to ship emissions coupled to extensive cloud cover in the study region is beneficial for converting micronutrients to soluble forms.
(4) Measurements of tracer elements with crustal and anthropogenic origins (Si, B, Cs) point to influence from continental particle types (e.g., fly ash, crustal matter) impacting stratocumulus clouds off the California coast.

Acknowledgments

This work was funded by ONR grants N00014-11-1-0783, N00014-10-1-0200, and N00014-10-1-0811, and NSF grant AGS-1008848. We acknowledge Dean Hegg for providing the cloud water collector and Lindsay C. Maudlin for comments on the draft. The authors gratefully acknowledge the NOAA Air Resources Laboratory (ARL) for the provision of the HYSPLIT transport and dispersion model and READY website (http://ready.arl.noaa.gov) used in this publication.

Appendix A. Supplementary data

Supplementary data related to this article can be found at http://dx.doi.org/10.1016/j.atmosenv.2014.01.020.

References

Alexander, B., Park, R.J., Jacob, D.J., Gong, S.L., 2009. Transition metal-catalyzed oxidation of atmospheric sulfur: global implications for the sulfur budget. J. Geophys. Res. 114, D02309. http://dx.doi.org/10.1029/2008JD010486.

Al-Momani, I.F., 2003. Trace elements in atmospheric precipitation at Northern Jordan measured by ICP-MS: acidity and possible sources. Atmos. Environ. 37, 4507–4515.

Benedict, K.B., Lee, T., Collett Jr., J.L., 2012. Cloud water composition over the Southeastern Pacific Ocean during the VOCALS regional experiment. Atmos. Environ. 46, 104–114.

Capone, D.G., Hutchins, D.A., 2013. Microbial biogeochemistry of coastal upwelling regimes in a changing ocean. Nat. Geosci. 6, 711–717.

Chen, Y.C., et al., 2012. Occurrence of lower cloud albedo in ship tracks. Atmos. Chem. Phys. 12, 8223–8235.

Coggon, M.M., et al., 2012. Ship impacts on the marine atmosphere: insights into the contribution of shipping emissions to the properties of marine aerosol and clouds. Atmos. Chem. Phys. 12, 8439–8458.

Collett, J.L., et al., 2002. The chemical composition of fogs and intercepted clouds in the United States. Atmos. Res. 64, 29–40.

Crahan, K.K., Hegg, D., Covert, D.S., Jonsson, H., 2004. An exploration of aqueous oxalic acid production in the coastal marine atmosphere. Atmos. Environ. 38, 3757–3764.

Draxler, R.R., Rolph, G.D., 2012. HYSPLIT (HYbrid Single-Particle Lagrangian Integrated Trajectory) Model. NOAA Air Resources Laboratory, Silver Spring, MD. http://ready.arl.noaa.gov/HYSPLIT.php.

Enami, S., Vecitis, C.D., Cheng, J., Hoffmann, M.R., Colussi, A.J., 2007. Global inorganic source of atmospheric bromine. J. Phys. Chem. A 111, 8749–8752. http://dx.doi.org/10.1021/JP074903R.

Furutani, H., Jung, J., Miura, K., Takami, A., Kato, S., Kajii, Y., Uematsu, M., 2011. Single-particle chemical characterization and source apportionment of iron-containing atmospheric aerosols in Asian outflow. J. Geophys. Res. 116, D18204. http://dx.doi.org/10.1029/2011JD015867.

Galloway, J.N., et al., 2004. Nitrogen cycles: past, present, and future. Biogeochemistry 70, 153–226.

Gerber, H., Arends, B.G., Ackerman, A.S., 1994. New microphysics sensor for aircraft use. Atmos. Res. 31, 235–252.

Gioda, A., Mayol-Bracero, O.L., Reyes-Rodriguez, G.J., Santos-Figueroa, G., Collett, J.L., 2008. Water-soluble organic and nitrogen levels in cloud and rainwater in a background marine environment under influence of different air masses. J. Atmos. Chem. 61, 85–99. http://dx.doi.org/10.1007/S10874-009-9125-6.

Hegg, D.A., Hobbs, P.V., 1986. Sulfate and nitrate chemistry in cumuliform clouds. Atmos. Environ. 20, 901–909. http://dx.doi.org/10.1016/0004-6981(86)90274-X.

Hegg, D.A., Gao, S., Jonsson, H., 2002. Measurements of selected dicarboxylic acids in marine cloud water. Atmos. Res. 62, 1–10. http://dx.doi.org/10.1016/S0169-8095(02)00023-6.

Hegg, D.A., Covert, D.S., Jonsson, H., Covert, P.A., 2005. Determination of the transmission efficiency of an aircraft aerosol inlet. Aerosol Sci. Technol. 39, 966–971. http://dx.doi.org/10.1080/02786820500377814.

Hegg, D.A., Covert, D.S., Jonsson, H.H., Woods, R.K., 2010. The contribution of anthropogenic aerosols to aerosol light-scattering and CCN activity in the California coastal zone. Atmos. Chem. Phys. 10, 7341–7351. http://dx.doi.org/10.5194/acp-10-7341-2010.

Jickells, T.D., et al., 2005. Global iron connections between desert dust, ocean biogeochemistry, and climate. Science 308, 67–71. http://dx.doi.org/10.1126/science.1105959.

Johansen, A.M., Siefert, R.L., Hoffmann, M.R., 1999. Chemical characterization of ambient aerosol collected during the southwest monsoon and intermonsoon seasons over the Arabian Sea: anions and cations. J. Geophys. Res.-Atmos. 104, 26325–26347.

Johnson, K.S., Gordon, R.M., Coale, K.H., 1997. What controls dissolved iron concentrations in the world ocean? Mar. Chem. 57, 137–161.

Kirchman, D.L., Meon, B., Cottrell, M.T., Hutchins, D.A., Weeks, D., Bruland, K.W., 2000. Carbon versus iron limitation of bacterial growth in the California upwelling regime. Limnol. Oceanogr. 45, 1681–1688.

Krishnamurthy, A., et al., 2009. Impacts of increasing anthropogenic soluble iron and nitrogen deposition on ocean biogeochemistry. Glob. Biogeochem. Cycles 23, GB3016. http://dx.doi.org/10.1029/2008GB003440.

Lammel, G., Metzig, G., 1998. On the occurrence of nitrite in urban fogwater. Chemosphere 37, 1603–1614.

Luo, C., et al., 2005. Estimation of iron solubility from observations and a global aerosol model. J. Geophys. Res.-Atmos. 110, D23307. http://dx.doi.org/10.1029/2005JD006059.

Meskhidze, N., Chameides, W.L., Nenes, A., 2005. Dust and pollution: a recipe for enhanced ocean fertilization? J. Geophys. Res. 110, D03301 http://dx.doi.org/10.1029/2004JD005082.

Moore, R.M., Milley, J.E., Chatt, A., 1984. The potential for biological mobilization of trace-elements from aeolian dust in the ocean and its importance in the case of iron. Oceanol. Acta 7, 221–228.

Mueller, D., Uibel, S., Takemura, M., Klingelhoefer, D., Groneberg, D.A., 2011. Ships, ports and particulate air pollution – an analysis of recent studies. J. Occup. Med. Toxicol. 6 (31). http://dx.doi.org/10.1186/1745-6673-6-31.

Murphy, S.M., et al., 2009. Comprehensive simultaneous shipboard and airborne characterization of exhaust from a modern container ship at sea. Environ. Sci. Technol. 43, 4626–4640. http://dx.doi.org/10.1021/ES802413J.

Nriagu, J.O., 1989. A global assessment of natural sources of atmospheric trace metals. Nature 338, 47–49. http://dx.doi.org/10.1038/338047A0.

Popovicheva, O., et al., 2009. Ship particulate pollutants: characterization in terms of environmental implication. J. Environ. Monit. 11, 2077–2086. http://dx.doi.org/10.1039/B908180A.

Popovicheva, O., Kireeva, E., Persiantseva, N., Timofeev, M., Bladt, H., Ivleva, N.P., Niessner, R., Moldanova, J., 2012. Microscopic characterization of individual particles from multicomponent ship exhaust. J. Environ. Monit. 14, 3101–3110.

Russell, L.M., et al., 2013. Eastern Pacific Emitted Aerosol Cloud Experiment (E-PEACE). Bull. Am. Meteorol. Soc. 94, 709–729.

Seinfeld, J.H., Pandis, S.N., 2006. Atmospheric Chemistry and Physics, second ed. Wiley-Interscience, New York.

Shi, Z.B., Krom, M.D., Bonneville, S., Baker, A.R., Jickells, T.D., Benning, L.G., 2009. Formation of iron nanoparticles and increase in iron reactivity in mineral dust during simulated cloud processing. Environ. Sci. Technol. 43, 6592–6596. http://dx.doi.org/10.1021/ES901294G.

Shingler, T., et al., 2012. Characterisation and airborne deployment of a new counterflow virtual impactor inlet. Atmos. Meas. Tech. 5, 1259–1269. http://dx.doi.org/10.5194/amt-5-1259-2012.

Sholkovitz, E.R., Sedwick, P.N., Church, T.M., 2009. Influence of anthropogenic combustion emissions on the deposition of soluble aerosol iron to the ocean: empirical estimates for island sites in the North Atlantic. Geochim. Cosmochim. Acta 73, 3981–4003. http://dx.doi.org/10.1016/j.gca.2009.04.029.

Singh, R.P., Prasad, A.K., Kayetha, V.K., Kafatos, M., 2008. Enhancement of oceanic parameters associated with dust storms using satellite data. J. Geophys. Res.-Oceans 113, C11008. http://dx.doi.org/10.1029/2008JC004815.

Sorooshian, A., et al., 2010. Constraining the contribution of organic acids and AMS m/z 44 to the organic aerosol budget: on the importance of meteorology, aerosol hygroscopicity, and region. Geophys. Res. Lett. 37, L21807. http://dx.doi.org/10.1029/2010GL044951.

Sorooshian, A., et al., 2012. Hygroscopic and chemical properties of aerosols collected near a copper smelter: implications for public and environmental health. Environ. Sci. Technol. 46, 9473–9480.

Sorooshian, A., Wang, Z., Coggon, M.M., Jonsson, H.H., Ervens, B., 2013. Observations of sharp oxalate reductions in stratocumulus clouds at variable altitudes: organic acid and metal measurements during the 2011 E-PEACE campaign. Environ. Sci. Technol. 47, 7747–7756. http://dx.doi.org/10.1021/es4012383.

Straub, D.J., Lee, T., Collett Jr., J.L., 2007. Chemical composition of marine stratocumulus clouds over the Eastern Pacific Ocean. J. Geophys. Res.-Atmos. 112, D04307. http://dx.doi.org/10.1029/2006JD007439.

Viana, M., et al., 2009. Chemical tracers of particulate emissions from commercial shipping. Environ. Sci. Technol. 43, 7472–7477.

Wonaschuetz, A., et al., 2013. Hygroscopic properties of smoke-generated organic aerosol particles emitted in the marine atmosphere. Atmos. Chem. Phys. 13, 9819–9835.

Xie, Z.Q., Blum, J.D., Utsunomiya, S., Ewing, R.C., Wang, X.M., Sun, L.G., 2007. Summertime carbonaceous aerosols collected in the marine boundary layer of the Arctic Ocean. J. Geophys. Res.-Atmos. 112, D02306. http://dx.doi.org/10.1029/2006JD007247.

Zhuang, G., Duce, R.A., Kester, D.R., 1990. The dissolution of atmospheric iron in surface seawater of the open ocean. J. Geophys. Res. 95, 16207–16216.

Zhuang, G.S., Yi, Z., Duce, R.A., Brown, P.R., 1992. Chemistry of iron in marine aerosols. Glob. Biogeochem. Cycles 7 (2), 161–173. http://dx.doi.org/10.1029/92GB00756.

Zuo, Y.G., Hoigne, J., 1992. Formation of hydrogen-peroxide and depletion of oxalic-acid in atmospheric water by photolysis of iron(iii) oxalato complexes. Environ. Sci. Technol. 26, 1014–1022.